

Ductility-based Performance Design and Research of Cable-net Substructure plus Major Steel Structure for the Art Wall of Henan Province Art Centre

Jiaqi Ge



Jiaqi Ge*, Ling Zhang*, Shu Wang*, Jiyang Huang*, Bin Wang*

* China Aeronautical Project and Design Institute,

Abstract

The art wall, 40m high with a part of cantilevered height on the top at Henan Art Centre, adopts a structural system of the major steel structure of in-plane penetrated welded steel pipe truss reinforced by the single-layer cable-net substructure on both sides of the truss. Firstly, structural overall stability analysis and design are conducted by considering geometric nonlinearity, elastic-plastic material, and initial geometric imperfection, to identify yield ratio and ductile deformation of the structural system under the limit state of large deformation buckling collapse. Furthermore, the structural earthquake-resistant performance is studied on the basis of ductility behavior by performing an elastic-plastic time-history analysis for the whole structure, and then in-depth quantification analysis and design are conducted to obtain the structure's modal, stress ratio of members, displacement, distribution of plastic hinge, and damage level. According to above series of analysis and research, the objective of double ductility performance designs of overall stability safety and earthquake-resistant security respectively is achieved.

Keywords: ductility performance; geometric nonlinearity; overall stability buckling analysis; elasto-plastic time-history analysis

1. Introduction

Henan Province Art Centre, located in the central business district of Zhengdong New Zone, is composed of seven building units in total, mainly including theater, concert hall and public hall. The art wall of public hall is a quintessential part of the art of architectural modeling (Ge and Wang, 2008).

The art wall, 166m long with top elevation of 39.68m and bottom elevation of 8.47m, is built up of a longitudinal major in-plane truss with a slope angle of 78 degrees and a horizontal in-plane truss. The top and bottom chords of the longitudinal truss are connected with the foundation by pin roll. Within the large square grid (approximate $8.4\text{m} \times 3.0\text{m}$) formed by the longitudinal and horizontal truss, the single-layer cable-net is applied to mesh the grid to the dimension of $2.1\text{m} \times 1.5$ on both sides of the truss, and material of glass is installed in every meshed grid (Technical Code of Glass Curtain Wall Engineering, 2003) (See Figure 1). The longitudinal cables are primarily stressed, producing a load transfer path in the shape of “ Γ ” around the art wall (See Figure 1) with a larger pre-stressing of 80~120kN, while the transverse cables are for stability

applied to 20kN pre-stressing.

2. Objective of structural ductility-based performance design and computational model

2.1 Objective of ductility-based performance design

Based on the former engineering research results and the engineering characteristics of curtain wall, the aims of structural engineering safety of ductility performance design are as follows:

- (1) When geometric nonlinear analysis is conducted, the maximum elastic deformation of the structural system, subject to minor seismic and static loads, including wind load, shall not be more than 1/400 of the span or height of the structure (Ge and Zhang, 2007);
- (2) When elasto-plastic geometric nonlinear analysis is performed, the stability bearing capacity factor of the structural system, subject to static allowable load combinations, including wind load, shall be more than 2.5 (Ge and Zhang, 2007);
- (3) When elasto-plastic geometric nonlinear analysis is performed, the large deformation of the structural

system, subject to ultimate seismic load combinations, including wind load, shall be less than 1/50 of the span or height of the structure, and the cable element shall keep elastic (Xie and Zhai, 2003);

- (4) When elasto-plastic geometric nonlinear analysis is performed, the end connection, subject to ultimate seismic load combinations, including wind load, shall remain elastic. Specifically, the finite element analysis of the end connection shall be conducted to obtain three fully-step curves, namely load-stress, load-strain, and load-displacement, of which the minimum stability capacity is considered to be the bearing capacity of the end connection (Xie and Zhai, 2003). Additionally, it's required to be larger than the reaction of the end connection subject to ultimate seismic load combinations or structural buckling load combinations.

2.2 Structural computational model

In order to study the impact of coincident work between the cable-net substructure and the major structure of the art wall on the whole structure, four types of the computational models are introduced. Model 1 contains the art wall plus the cable-net substructure, Model 2 is the art wall without the cable-net substructure, Model 3 consists of the art wall plus the cable-net substructure and the public hall, and Model 4 is comprised of the art wall plus the public hall without the cable-net substructure. The first two models are adopted for stability analysis; the latter two models are utilized for seismic performance analysis.

The computation is implemented by using ANSYS General Finite Element Analysis Package, in which beam element of Beam188 is used for the chords of the major steel truss, truss element of Link8 is for the web members, and tension-only spar element of Link10 is for the cables. Material of Q235 steel is employed for the web members of the major steel truss, while Q345 steel is for the other steel members. The whole structural model is shown in Figure 1.

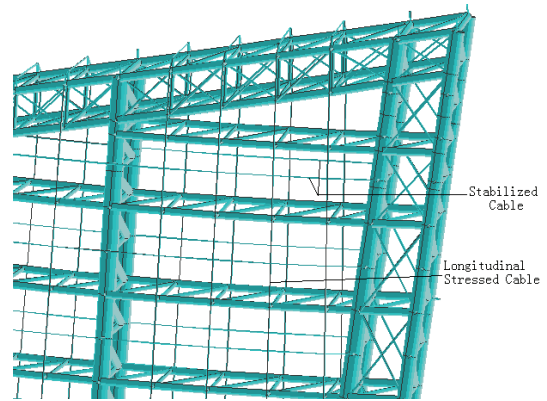
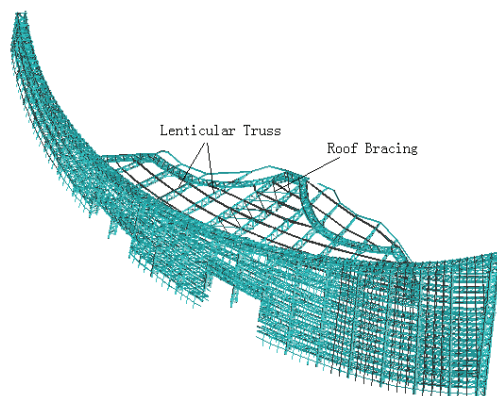


Figure 1 Structural Model

3. Stability performance analysis of the whole structure

As shown in the analysis results of Ge and Wang (2008), the first five buckling modes of the structure are all related to an out-of-plane instability of the lenticular (fish-bellied) truss of the public hall. In order to study the pre-stressing system's impact on the major steel truss and avoid the effect of the public hall on the computation results, the fixed pin connections are used between the art wall and the public hall in Model 1 and Model 2. The different analyses are performed respectively, including linear eigen-value buckling analysis, geometric nonlinear stability analysis, and elasto-plastic geometric nonlinear stability analysis. The variable load combinations are adopted for structural strength and serviceability designs in accordance with local codes, while for structural stability design, the load combination of (1.0 dead load + 1.0 live load + 0.7 wind load) is introduced (Shen and Chen, 1999).

3.1 Linear eigen-value buckling analysis

The linear buckling analysis results are illustrated in Figure 2.

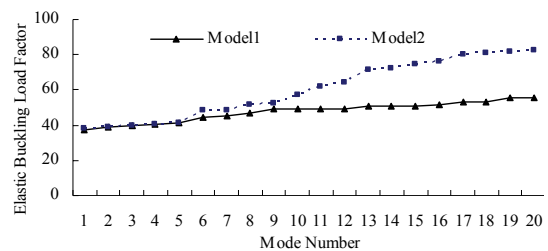


Figure 2 Comparison of the Linear Buckling Analysis Results

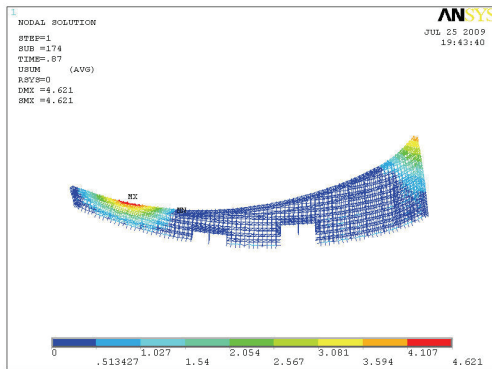
It can be seen from the structural eigen-value calculation results:

- (1) In both Model 1 and Model 2, the first five eigen-values of are close, approximately 35.0, of which the buckling modes are basically same and are mainly regarded as the out-of-plane partial buckling of the major truss of the art wall;
- (2) However, it begins that the sixth buckling mode

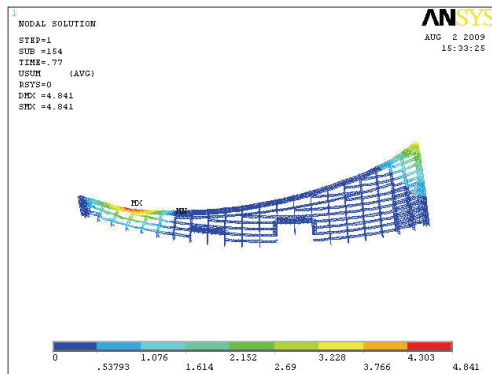
becomes different between two models. The sixth buckling mode of Model 1 is mainly on the out-of-plane cable-net substructure, while the out-of-plane buckling of the major truss occurs in the sixth mode in Model 2. Furthermore, the sixth eigen-value and the followings of Model 1 are gradually larger than that of Model 2, which explains that the cable-net substructure plays a helpful role on increasing the structural stability.

3.2 Geometric nonlinear structural stability analysis

By considering structural initial geometric imperfection and geometric nonlinearity, utilizing uniform deviation mode method, that is to say, the structural fundamental buckling mode (first mode) is employed for the imperfection configuration, and applying 1/300 of the wall height as a geometric imperfection magnitude to the imperfection configuration (Latticed Shell Structure Technology Standards, 2003), the calculation results for Model 1 and Model 2 are shown in Figures 3, 4 and 5.



(a) Model 1



(b) Model 2

Figure 3 Structural Buckling Displacements

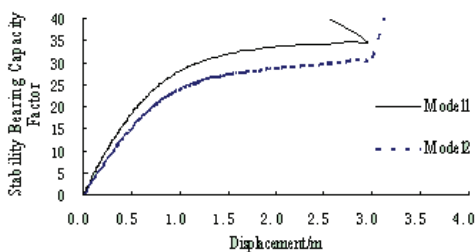


Figure 4 Load-displacement Curves of the Nodes with the Maximum Buckling Displacement

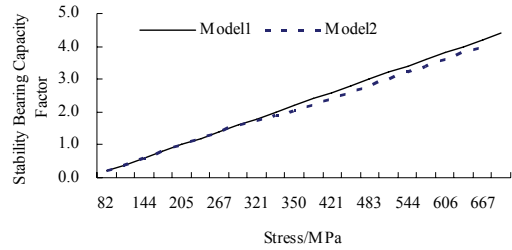


Figure 5 Load-stress Curves of the Nodes with the Maximum Buckling Displacement

As shown in above calculation results:

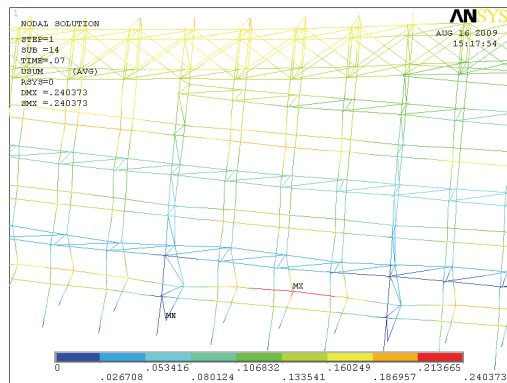
- (1) By comparing above calculation results, the structural buckling behaviors of both two models are the out-of-plane instability of the transverse in-plane truss, and the stability bearing capacity factor are 30.0 for Model 1 and 25.0 for Model 2 respectively. Besides, when the structure stays in buckling, the maximum horizontal displacement of Model 1 is 1.20m (1/7.0 of the corresponding wall height), while the displacement is 1.10m (1/7.6 of the height) for Model 2. As a result, the cable-net substructure plays a positive role on structural overall stability; and the structural stability bearing capacity factor of Model 1 is raised by 13%, compared to Model 2.
- (2) As can be seen in the load-stress curves of the nodes on the transverse in-plane truss chords, when the load multiple in Model 1 reaches 2.0, the member strength goes to yield stress 345MPa, while when the load time in Model 2 is 1.9, the member strength comes to yield stress 345MPa. Before the structural system arrives at stability bearing capacity, the members already yield.
- (3) When the large deformation limit 1/50 (0.17m) is taken as the performance objective (Code for design of Steel Structure, 2008), the system stability bearing capacity factor is 7.5 for Model 1 and 6.0 for Model 2. Even though it happens, the members already yield based on Figure 5. Therefore, these stability bearing capacity factors cannot reflect the real structural stability performance.

To sum up, although the system stability bearing capacity factors achieve 30.0 and 25.0 by only conducting geometric nonlinear analysis, the members are already destroyed, of which the system displacement is more than 1/10, and actually the structure stays in collapse. Therefore, elasto-plastic geometric nonlinearity shall be considered in stability analysis of the in-plane truss oriented structural system, and there is nothing to do with the engineering reality for the in-plane truss oriented structural system by only considering geometric nonlinearity.

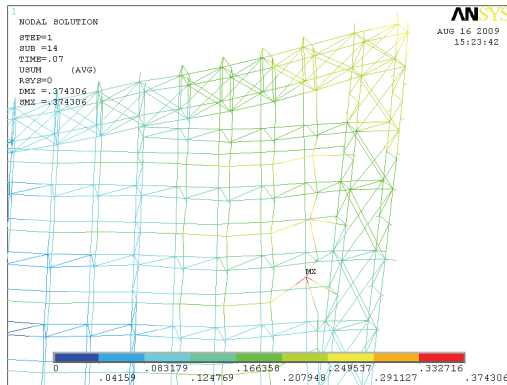
3.3 Elasto-plastic geometric nonlinear structural stability

analysis

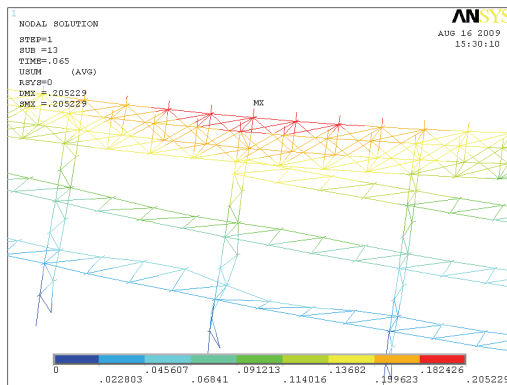
By considering elasto-plastic geometric nonlinearity, the main calculation results of structural stability analysis are shown in Figures 6 and 7.



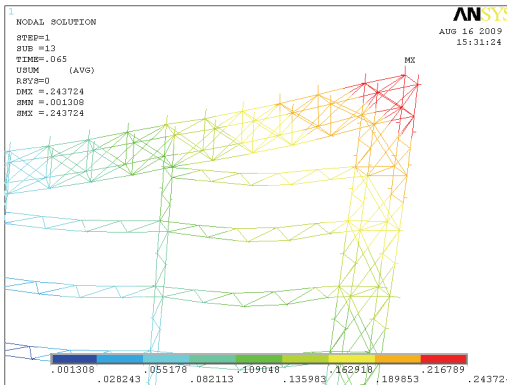
Model 1 Short Wall



Model 1 High Wall



Model 2 Short Wall



Model 2 High Wall

Figure 6 Comparison of the Structural Buckling Displacements

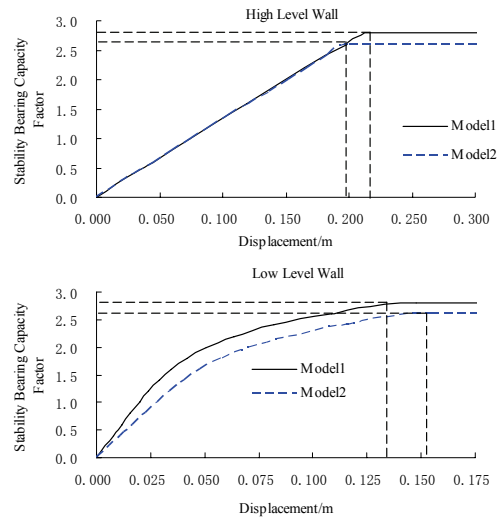


Figure 7 Load-displacement Curves of the Nodes with the Maximum Buckling Displacement

As shown in above calculation results:

- (1) As considering elasto-plastic geometric nonlinearity, both Model 1 and Model 2 have the same buckling behavior that the transverse in-plane trusses of the short walls goes to out-of-plane buckling.
- (2) The stability bearing capacity factors are 2.8 for Model 1 and 2.6 for Model 2 respectively. When Model 1 goes to buckling, the maximum horizontal displacement of the high wall is 219mm (1/183 of the corresponding wall height) and the short wall has the displacement of 141mm (1/64 of the wall height), while for Model 2, the displacement of the high wall is 204mm (1/196) and the short wall owns the displacement of 154mm (1/54).
- (3) After some local members become plastic in Model 1, the stability bearing capacity factor is 2.0; and then increases by 40% to 2.8.
- (4) The cable-net substructure can strengthen structural safety capacity, and the stability bearing capacity factor enhances by 8%, compared to without the cable-net substructure. Based on the structural load-displacement curves, because the high wall is thick, the pre-stressed cables around the thick wall have little impact on structural rigidity, and the displacement of the high wall in Model 1 is not clearly different from that of Model 2. For the short wall, when the load multiple is 2.6, the displacement in Model 1 is only 116mm, about 25% decreased compared to that of Model 2, so that the pre-stressed cables around the short wall cause a great impact on the structural buckling large deformation.
- (5) When considering elasto-plastic geometric nonlinearity, Model 1, reflecting actual engineering conditions, owns the maximum horizontal

displacement of $141\text{mm}/8400\text{mm}=1/64$ (less than $1/50$), and the maximum stress of the longitudinal cable is 563.2MPa and 89.7MPa for the transverse cable, which meet the ductility performance design objective.

4. Earthquake-resistant performance analysis of the

Table 1. Modal Analysis (1st~10th Period /s)

Modal	1	2	3	4	5	6	7	8	9	10
Model 3	1.3699	1.5873	1.8868	2.1739	2.2727	2.3256	2.3810	2.6316	2.7027	2.9412
Model 4	1.4057	1.6107	1.8499	2.2008	2.2710	2.2996	2.3951	2.5974	2.6358	2.9420

Through modal analysis for Model 3 and Model 4, it is concluded that: (1) the first three modals of both models are out-of-plane vibration of the lenticular truss of the public hall, and from the fourth modal, the integral translation occurs between the art wall and the public hall; (2) the cable-net substructure does not perform an obvious impact on self-vibration behavior of the major structure, due to lower rigidity of the cable-net substructure than that of the major structure.

4.2 Structural elasto-plastic time-history analysis under ultimate (seldom occurred) earthquake

MIDAS Finite Element Analysis Package is used for dynamic elasto-plastic time-history analysis, and because the cable-net substructure has little impact on self-vibration behavior of the major structure and the cable-net structure is less impacted by earthquake, Model 4 is selected for an earthquake-resistant performance analysis under ultimate earthquake. The rules of overall structural mechanical response and safety performance are mainly reviewed under ultimate earthquake. The ultimate earthquake load is generated by the mass from the gravity representative value (1.0dead load + 0.5live load) times the accelerations of three different directions, a_x , a_y and a_z , with the ratio of $a_x : a_y : a_z = 1 : 0.85 : 0.65$ (Code for Seismic Design of Buildings, 2008). For this project, engineering earthquake-resistant fortification intensity is 7 (0.15g), site category is III, and the building

structural system

4.1 Structural dynamic behavior

The structural natural periods are shown in Table 1. The modal shape figures are not illustrated here due to the limited pages of this paper.

belongs to Class B (Code for Seismic Design of Buildings, 2008). In the design, calculation and analysis of the structural dynamic response are conducted by inputting two series of natural seismic waves and one series of man-made seismic wave respectively. Due to the page limit, the structural mechanical performance results are listed below under only one series of three dimensional earthquake loads of 1940 EL Centro wave.

4.2.1 Calculation results of structural dynamic response under ultimate earthquake

The structural displacements and total end reactions are tabulated in Table 2. The plastic hinge distribution results are shown in Figure 8 under ultimate earthquake load of fortification intensity 9.

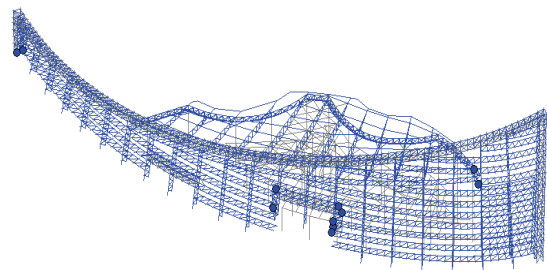


Figure 8 Structural Plastic Hinge Distribution

Table 2. Calculation Results of the Structural Displacement and Total End Reaction

Earthquake fortification Intensity	Displacement (mm)				Maximum End Reaction (kN)			
	Maximum Out-of-plane Displacement of the Lenticular Truss	Displacement of the Highest Node of the Art Wall $u_{x\max}$	Maximum Displacement of the Art Wall		F_x	F_y	F_z	
			$u_{x\max}$	$u_{y\max}$			Compression	Pulling Force
7	23	69	122	37	1007	1081	6982	6011
8	38	94	191	59	1542	1731	10186	9141
9	46	107	228	72	1837	2089	11962	10873

As shown in above figure and table:

(1) The members of the art wall remain elastic under

ultimate earthquake load of fortification intensity 7, which means the structure owns a good earthquake resistant performance.

- (2) In order to locate the structural weak positions, an elasto-plastic time-history analysis is conducted by increasing fortification intensity to 8 and 9 to enlarge the acceleration based on Chinese code of seismic design of buildings. Under fortification intensity 9, the plastic hinges occur at the structural weak positions (See Figure 8). However, because these plastic hinges belong to Class 1 (Chen, 2001), the members are at the beginning of yield state, of which the weakness degree is not high. Therefore, the art wall possesses a reasonable safety performance under ultimate earthquake load of fortification intensity 9.
- (3) According to the structural dynamic behavior results in Clause 4.1, out-of-plane rigidity of the lenticular truss is relatively weak. One of the lenticular trusses with the maximum span is selected for further analysis. As tabulated in Table 2, the out-of-plane displacements of the lenticular truss are 1/117, 1/71, and 1/59 (less than 1/50) of the span respectively under three different fortification intensities, which

meet the earthquake-resistant performance objective.

- (4) Because out-of-plane rigidity of the spatial truss around the high wall is relatively large, the horizontal displacement at the highest point of the structure is not the largest, while the visible structural horizontal displacement happens on the top of the fourth longitudinal in-plane truss on the left of the high wall. Under three different fortification intensities, the horizontal displacements are 1/245, 1/157, and 1/131 (less than 1/50) of the wall height at X direction, and 1/810, 1/508, and 1/417 (less than 1/50) at Y direction, which meet the earthquake-resistant performance objective.

5. Ductility performance analysis of the key connection

5.1 Distribution contour of the connection's equivalent stress and strain

The maximum reaction of the end connections is listed in Table 3 under structural overall buckling and ultimate earthquake respectively, of which the larger values are selected for the design load of the end connection.

Table 3. Maximum Reaction of the End Connection

Control Force	Structural Buckling		Ultimate Earthquake		Design Load for end connection	
	Compression -bending	Tension -bending	Compression -bending	Tension -bending	Compression -bending	Tension -bending
Axial Force F /kN	-10740	7069	-6586.4	6113.4	-10740	7069
Bending Moment M /kN·m	44.25	51.31	23.2	36.6	44.25	51.31

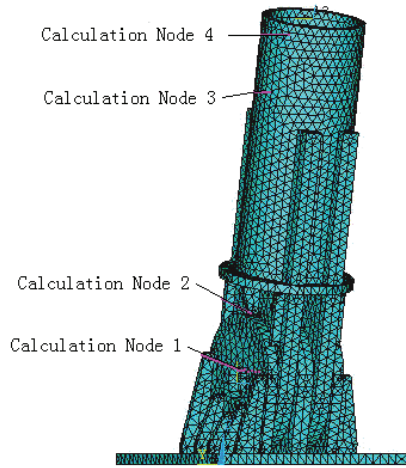
Finite element analysis is conducted for the key end connection, in which 8-node Solid45 element is used for solid modeling of the connection in ANSYS. The finite element model is meshed automatically to obtain more than 30,000 elements (See Figure 9). According to the results from structural buckling analysis and ultimate seismic analysis respectively, the forces from the member end connected to the end connection are extracted in the critical load combination, and then their equivalent reactions are applied to the other top end of the member in the finite element model. In response to Saint-Venant Principle, this type of equivalent loads has little impact on the end connection's stress far from the applied load (Chen, 2001). The nodes around the pin roll on the upper and lower parts of the end connection are coupled in the cylindrical coordinate of translation R (radius of pin roll) and Z (axis of pin roll), and released of the angles (θ) of rotation, in order to ensure only pinned rotation of the both parts and simulate the rotational delivery performance of the pin roll. Because there is no translation at the bottom of the connection, the bottom face translation of the end plate of the connection is fixed to display a real boundary condition of the connection. Q345 steel grade is used for the elements, as well as the

ideal elasto-plastic model and Von Mises yielding criteria are employed to simulate the material.

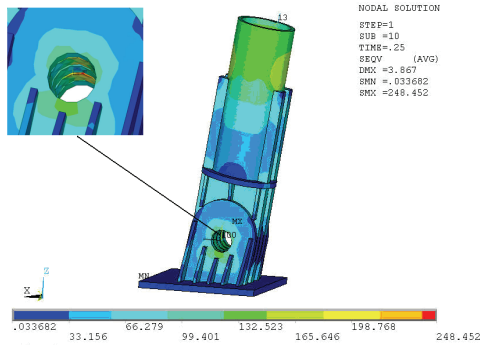
In Figure 9, Calculation node 1 of the model is chosen in the maximum stress zone of the pin roll in the upper part of the end connection, around which the elements go to yield at first; calculation node 2 is close to the pin roll underneath the stiffener in the upper part of the end connection; calculation nodes 3 and 4 are on the pipe with a large stress zone. Four nodes are all on one side of the pipe with a large stress in the upper part of the end connection subject to bending action. The calculation results are shown in Figure 10.



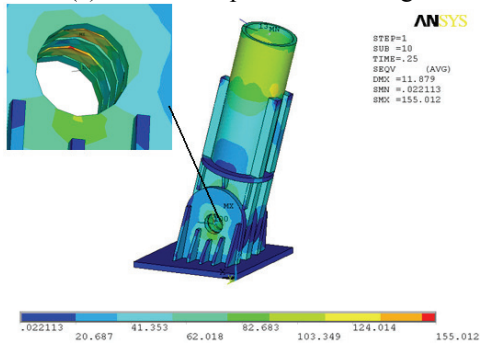
a) Real Photo



(b) Finite Element Model
Figure 9 End Connection



(a) Under Compression-bending



(b) Under Tension-bending

Figure 10 Von Mises Stress Distribution Contour

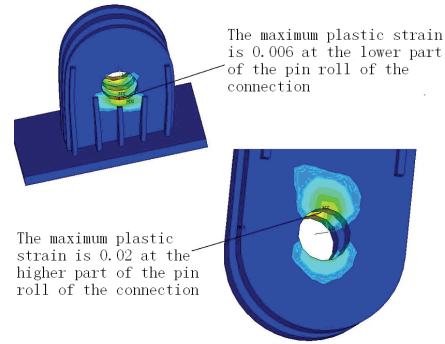
When the pipe top is applied with axial force and bending moment perpendicular to the axis of the pin roll, its stress behavior under structural overall buckling loads is as follows:

- (1) According to the Von Mises stress contour, when subject to compression-bending, the maximum stress, 248MPa, occurs on the compression side of the pin roll in the upper part of the end connection, while the maximum stress is 155MPa on the compression side of the same place subject to tension-bending.
- (2) Under the design loads, compression-bending and tension-bending each, the end connection does not

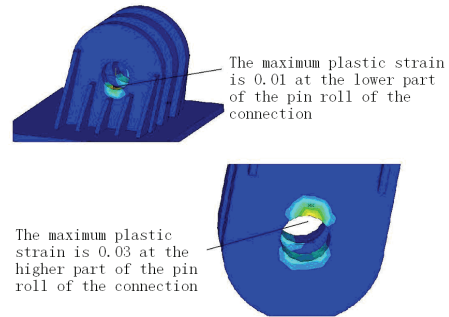
appear plastic development zone and remains elastic.

5.2 Distribution contour of the connection's equivalent stress and strain after multiplying the design load

To further analyze the stress behavior of the end connection under compression-bending and tension-bending respectively, the design load is increased 4 times to conduct finite element analysis, and then to observe the plastic development performance, of which the results are shown in Figure 11.



(a) Plastic Strain under Compression-bending when Calculation Terminates



(b) Plastic Strain under Tension-bending when Calculation Terminates

Figure 11 Strain Distribution Contour

As shown in the results, the large stress location is on the top area of the stiffener on the compression side of the upper pipe member. When the loads are 1.6~2 times larger than the design load, the plastic development area happens only around the upper pin roll of the end connection firstly, the lower support does not appear plastic strain.

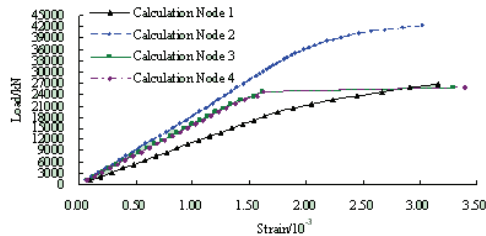
When the load continues increasing, the plastic development area firstly expands on the upper pin roll, and plasticity grows immediately, after that the lower pin roll displays plastic strain. Above analysis shows that the stiffeners well limit the expansion of plastic area even though the lower support goes into plasticity, and the plastic range is not much. Therefore, it is important that the stiffeners are applied in the structural ductility design and shall be emphasized in the structural steel design.

In conclusion, when the end connection is subject to buckling and ultimate earthquake each, the maximum plastic strain development area occurs on the top of the

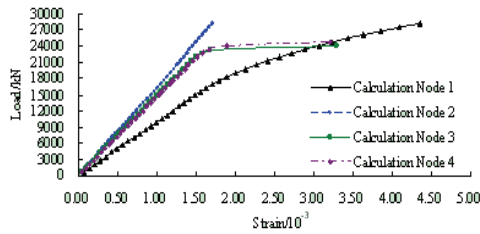
upper pin roll of the end connection, which shall be strengthened in the structural ductility design.

5.3 Load-stress / strain analysis of the end connection

In elasto-plastic finite element analysis of the connection, the typical calculation nodes on the pin roll and pipe staying in buckling are selected to calculate the load-stress/strain curves (See Figure 12).



(a) Load-Strain Curves under Compression-bending



(b) Load-Strain Curves under Tension-bending

Figure 12 Load-Strain Full-step Curves

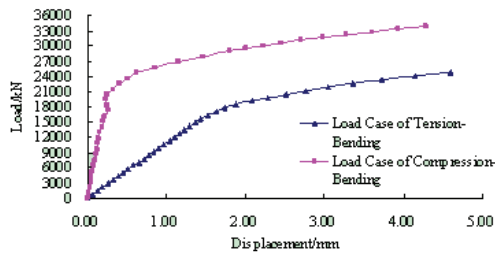


Figure 13 Load-Displacement Full-step Curves of Calculation Node 1

As shown in above diagrams:

- (1) Every calculation node has its own sequence to go to buckling collapse, of which the limit buckling loads are different. However, material becomes to yield when it comes to buckling with yield stress of $325\sim 345\text{N/mm}^2$ and yield strain of $0.015\sim 0.017$. It is demonstrated that the geometric configuration design of the connection is reasonable and their material strength is fully utilized when to stay in overall buckling.
- (2) The mechanical property of calculation node 1 is the weakest of the connection, which means this node becomes to buckling at first. The stability bearing capacity of node 1 is 16000kN under tension-bending and 17000kN under compression-bending, of which the stability bearing

capacity factor is 2.26 and 1.60 respectively.

In conclusion, when the load-stress/strain results of node 1 is considered as the security control objective for the end connection, because compression-bending is more critical than tension-bending, the stability bearing capacity is 17000kN and the stability bearing capacity factor is 1.60 for the whole end connection under compression-bending.

6. Conclusions

By above calculation and analysis, the main ductility performances of the structural steel art wall are as follows:

- (1) The reducing range of the stability bearing capacity factor for the in-plane truss structural system is much more than general spatial structures, provided only considering geometric nonlinearity is changed to consider elasto-plastic geometric nonlinearity. The deformation largely exceeds $1/50$ when the structural system is in the buckling state considering geometric nonlinearity, and the structure goes to buckling collapse. Therefore, the results just considering geometric nonlinearity cannot show the real stability performance of the structural system. Furthermore, for the structural steel system mainly comprised of in-plane truss, the method that the results from elastic analysis are divided by empirical coefficient in structural stability performance design is not safe enough.
- (2) By considering elasto-plastic geometric nonlinearity, the buckling behavior of the structural system is out-of-plane instability of the local transverse truss, of which the structural stability bearing capacity factor is 2.8 and the maximum horizontal displacement is $141\text{mm}/8400\text{mm}=1/64$ (less than $1/50$). Both yield ratio and ductile deformation of the structural system under the limit state of large deformation buckling collapse can meet the requirements of design.
- (3) The members of the art wall stay elastic under ultimate seismic load of fortification intensity 7. By increasing seismic acceleration, the calculation results show that the positions around the spatial truss around the door, the end connection of the low wall, and the connection between the spatial truss of the public hall and the main structure belong to the weak parts, but with a lower weakness level. Therefore, all these weak parts shall be reinforced to guarantee the structural safety.
- (4) The key end connections are designed in a reasonable configuration, so that the node elements do not have a local buckling collapse; the material strength capacity is fully utilized; the structure remains elastic without plastic development zone; the connections work safely. When a full-step buckling analysis is conducted, the upper part of the pin roll of the end connection starts to yield firstly and appears plastic strain. The existence of stiffeners effectively restricts the plastic development zone and

ensures the end connection safe. Therefore, the setup of stiffener shall be emphasized.

To sum up, when an elastic geometric nonlinear buckling analysis is performed, the structural overall stability bearing capacity factor is relatively high, while the structure already staying in the large deformation failure state is exhibited by the structural overall ductility performance coefficient (plastic displacement). It is proved that the overall stability design of ductility-based performance shall be comprised of the dual performance objectives of structural overall stability bearing capacity and deformation ductility performance, and then the safety can be ensured. In addition, the cables remain elastic under structural overall buckling and ultimate seismic action respectively. Furthermore, the art wall owns a mechanical character of “structural overall large deformation and cables with small strain”, which demonstrates that the cable elements with relatively low ductility performance display an adequate ductility safety performance in the structural system of this project.

References

- Code for design of Steel Structure[S], GB50017-2003.
- Code for Seismic Design of Buildings, GB50011-2001[S], 2008.
- Technical Code of Glass Curtain Wall Engineering, JGJ 102-2003.
- Chen S.F. “Steel Structure Design Theory [M]”, Beijing Science Press, 2001
- Ge J.Q. and Zhang G.J. (2007). “The Overall Stability Analysis of the Large-span Steel Structure for 2008 Olympic Games ”, Building Structure, No. 6, 22-30.
- Ge J.Q. and Wang S. (2008). “Performance Analysis and Design Research of the Structural Overall Stability of the Art Wall and Shared Hall of Henan Provincial Art Center”, Building Structure, No. 12, 11-13.
- Latticed Shell Structure Technology Standards [S], JGJ61-2003.
- Shen S.Z. and Chen X. “Stability of Latticed Shell [M]”, Beijing Science Press, 1999.
- Xie L.L. and Zhai C.H. (2003). “Study on the Severest Real Ground for Seismic Design and Analysis”, ACTA Seismologic Sinica, Vol. 25, No.3, 250-261.